First-principles study of elastic properties of CeO_2, ThO_2 and PoO_2

V Kanchana[1,2], G Vaitheeswaran[1,2], A Svane[3] and A Delin[2]

[1] Max-Planck-Institut für Festkörperforschung, Heisenbergstrasse 1, 70569 Stuttgart, Germany
[2] Department of Materials Science and Engineering, Royal Institute of Technology (KTH),
Brinellvägen 23, 100 44 Stockholm, Sweden
[3] Department of Physics and Astronomy, University of Aarhus, DK-8000 Aarhus C, Denmark

Abstract
Using first-principles density functional calculations, the structural and elastic
properties of fluorite type oxides CeO_2, ThO_2 and PoO_2 were studied by
means of the full-potential linear muffin-tin orbital method. Calculations were
performed within the local density approximation (LDA) as well as generalized
gradient approximation (GGA) to the exchange correlation potential. The
calculated equilibrium lattice constants and bulk moduli are in good agreement
with the experimental results, as are the computed elastic constants for CeO_2
and ThO_2. For PoO_2 this is the first quantitative theoretical prediction of the
ground state properties, and it still awaits experimental confirmation. The
calculations find PoO_2 to be a semiconductor with an indirect band gap and
elastic constants similar in magnitude to those of CeO_2 and ThO_2.

1. Introduction

Fluorite-type dioxides have attracted a great deal of interest from experimentalists as well
as theoreticians for the past two decades. The chemistry of these oxides is rather complex,
with the complications arising from the non-stoichiometry and often from the self-damage
resulting from the decay of the radioactive isotopes [1]. Nevertheless, numerous experimental
and theoretical studies have been carried out on these compounds. CeO_2 is one of the most
studied of the fluorite oxides [2–6]. Cerium dioxide is a technologically important material with
remarkable properties used in a number of applications. For instance, it is widely applied in
automobile exhaust catalysts as an oxygen storage material, due to its ability to take and release
oxygen under oxidizing and reducing conditions. Properties of ceria-based materials, such as
electrical conductivity and diffusivity, have been reviewed for its use as an electrolyte in solid
oxide fuel cells [7, 8]. ThO_2 is an example of an actinide oxide which crystallizes in the fluorite
structure. Both CeO_2 and ThO_2 are hard cubic oxides which have potential interests as optical
component materials and laser hosts [9], and numerous literature references are available for
these compounds investigating their electronic, bonding, optical, surface and ground state

properties [2–4, 10–14]. The valency of Ce in CeO_2 is still under debate. Two conflicting points of view, both based on the interpretation of core-level spectroscopy studies, describe the ground state as either tetravalent [15–17] or intermediate valent [18, 19]. However, recent self-interaction corrected local spin density total energy calculations on CeO_2 strongly suggest a tetravalent ground state [14]. Advancements in the field of high-pressure studies were also made for these compounds, revealing a pressure-induced structural phase transformation from the cubic fluorite structure to an orthorhombic structure of α-$PbCl_2$ type [20, 21]. In addition, Raman spectra at high pressure are also available for CeO_2 and ThO_2 which again confirm the high-pressure α-$PbCl_2$-type structure [22, 23]. Recently, the high-pressure behaviour of ThO_2 was reevaluated experimentally, and the value of the bulk modulus of ThO_2 at ambient pressure, which underwent a long debate, was finally settled [24, 25] and corroborated by theory [25].

From the perspective of materials science, the elastic constants C_{ij} contain some of the more important information which can be obtained from ground state total energy calculations. A given crystal structure cannot exist in a stable or a metastable phase unless its elastic constants obey certain relationships. The C_{ij} also determine the response of the crystal to external forces, as characterized by the bulk modulus, shear modulus, Young's modulus and Poisson's ratio, and so play an important role in determining the strength of the material. The elastic constants of CeO_2 and ThO_2 have been measured [26, 27], but theoretical calculations have been reported only for CeO_2 [28], which is one of the main objectives of the present work. For CeO_2 the experimental elastic constants were derived from the sound velocity for each acoustic phonon mode estimated from the frequency shift of Brillouin scattering lines [26]. For ThO_2 single-crystal elastic constants were determined by Macedo *et al* [27] by means of pulse echo technique.

A second objective of the present work is to study the compound PoO_2, which also crystallizes in the fluorite structure. Apart from the lattice constant, experimental information on this compound is scarce. Neither experimental nor theoretical details regarding the ground state properties, electronic structure, and elastic constants are available. Here, we present our theoretical results for PoO_2, including the electronic structure and the elastic constants, as obtained with the full-potential linear muffin-tin orbital method. We discuss the trends of the CeO_2, ThO_2 and PoO_2 fluorite oxides and compare with the available experimental results. The paper is organized as follows. Section 1 gives a brief introduction to the fluorite-type oxides and discusses the available literature on CeO_2, ThO_2 and PoO_2. Section 2 deals with the computational details, including the details regarding the calculation of elastic constants and Debye temperatures. Section 3 presents the results obtained, including discussion. Finally, section 4 contains the conclusions of the present work.

2. Computational details

2.1. The electronic structure method

In this work we have used the all-electron full-potential linear muffin-tin orbital (FP-LMTO) method [29] to calculate the total energies as well as the basic ground state properties. Here the crystal is divided into two regions: the non-overlapping muffin-tin spheres surrounding each atom and the interstitial region between the spheres. We used a double κ spdf LMTO basis (each radial function within the spheres is matched to a Hankel function in the interstitial region) for describing the valence bands. For Th and Po, the 6p states were included in the basis, and similarly, for Ce, the 5p states were used. Within the spheres, the potential is expanded in terms of spherical harmonics, while in the interstitial region, it is expanded in terms of plane waves. The exchange correlation potential was calculated both by the LDA [30] and the GGA

schemes [31]. The charge density and potential inside the muffin-tin spheres are represented by spherical harmonics up to $l_{max} = 6$, while in the interstitial region, 12 050 plane waves with energies up to 193.316 Ryd were included in the calculation. Total energies were calculated as a function of volume, with 413 k-points in the irreducible wedge of the Brillouin zone and fitted to the Birch equation of state [32] to obtain the ground state properties.

We have not included the spin–orbit coupling in our total energy calculations. This might seem a strange choice, considering that the spin–orbit coupling is significant in Ce, Th and Po. Our rationale for this is as follows. In a calculational method which uses a scalar relativistic ls basis, the relativistic p$_{1/2}$ states cannot be well described since they are nonzero at the origin, i.e., the Hilbert space spanned by the nonrelativistic basis set needs to be expanded in order to accommodate relativistic wavefunctions. One of the consequences of this fundamental shortcoming is that the equilibrium volume [33] is underestimated when the spin–orbit coupling is included. The correct way of dealing with this problem would of course be to develop a full-potential method based on a Dirac relativistic (j, κ) basis. With the lack of such a method, however, the problem can in fact to a large extent be avoided by simply ignoring the spin–orbit interaction altogether. This simple remedy results in larger theoretical equilibrium volume for light actinides and, consequently, better agreement with experiment [33]. The argument also holds for lanthanides with a shallow 5p shell, such as Ce.

2.2. The elastic constants

A cubic system has three independent elastic constants C_{11}, C_{12} and C_{44}. The bulk modulus B of this system can be expressed as a linear combination of C_{11} and C_{12}. The condition for elastic stability is that B, $C_{11} - C_{12}$, and C_{44} are positive [34]. The elastic constants can be obtained by calculating the total energy as a function of volume-conserving strains that break the cubic symmetry. For calculating C_{11} and C_{12}, we apply the tetragonal strain [35, 36] that transforms the lattice vectors as

$$\mathbf{R}' = \epsilon \mathbf{R}, \tag{1}$$

where $\mathbf{R}$ and $\mathbf{R}'$ are the old and new lattice vectors, respectively, and ϵ is the strain tensor expressed in terms of the tetragonal deformation parameter δ as

$$\epsilon_{\text{tet}} = \begin{pmatrix} 1+\delta & 0 & 0 \\ 0 & 1+\delta & 0 \\ 0 & 0 & 1/(1+\delta)^2 \end{pmatrix}. \tag{2}$$

Furthermore, the connection between the increase in total energy per unit cell volume, U, and the distortion, δ, is given by

$$U(\delta) = 6C'\delta^2 + \text{O}(\delta^3), \tag{3}$$

where C' is the tetragonal shear constant, which is also given by

$$C' = \tfrac{1}{2}(C_{11} - C_{12}). \tag{4}$$

By calculating C' and the bulk modulus

$$B = \tfrac{1}{3}(C_{11} + 2C_{12}) \tag{5}$$

from the Birch equation of state, the C_{11} and C_{12} parameters can be extracted.

Similarly, the following volume-conserving monoclinic strain [37] is applied to calculate C_{44}:

$$\epsilon_{\text{mon}} = \begin{pmatrix} 1 & \delta/2 & 0 \\ \delta/2 & 1 & 0 \\ 0 & 0 & 4/(4-\delta^2) \end{pmatrix}. \tag{6}$$

In this case, the strain energy density is even in the strain parameter and is given by

$$U(\delta) = \tfrac{1}{2}C_{44}\delta^2 + O(\delta^4). \tag{7}$$

The strain energy density is the increase of the energy density of a distorted system, which is proportional to the corresponding change in total energy. The accuracy of the total-energy differences needed for calculating the elastic constants is of the order of a microrydberg, and one needs a highly accurate computational method, like the FP-LMTO, to obtain a good agreement with experimental data.

C_{11}, C_{12}, and C_{44} comprise the complete set of elastic constants for a cubic system, and the shear modulus G, Young's modulus E, and the Poisson's ratio ν can be derived using the following relations:

$$G = \tfrac{1}{5}(3C_{44} + C_{11} - C_{12}), \tag{8}$$

$$E = \frac{9BG}{3B + G}, \tag{9}$$

$$\nu = \tfrac{1}{2}(1 - E/3B). \tag{10}$$

2.3. The Debye temperature

Having calculated the Young's modulus E, bulk modulus B, and shear modulus G, one can calculate the Debye temperature, which is an important fundamental parameter closely related to many physical properties such as elastic constants, specific heat and melting temperature.

At low temperatures the vibrational excitations arise solely from acoustic modes. Hence, at low temperatures the Debye temperature calculated from elastic constants is the same as that determined from specific heat measurements. One of the standard methods to calculate the Debye temperature (Θ_{D}) is from elastic constants data, since Θ_{D} may be estimated from the average sound velocity, v_{m} by the following equation [38]:

$$\Theta_{\mathrm{D}} = \frac{h}{k}\left[\frac{3}{4\pi}\left(\frac{N_{\mathrm{A}}\rho}{M}\right)\right]^{\frac{1}{3}} v_{\mathrm{m}}, \tag{11}$$

where h is Planck's constant, k is Boltzmann's constant, N_{A} is Avagadro's number, M is the molecular weight, and ρ is the density. Here we assume three acoustic branches contributing to the low-temperature specific heat. The average wave velocity is approximately calculated from [38]

$$v_{\mathrm{m}} = \left[\frac{1}{3}\left(\frac{2}{v_{\mathrm{s}}^3} + \frac{1}{v_{\mathrm{l}}^3}\right)\right]^{-\frac{1}{3}} \tag{12}$$

where v_{l} and v_{s} are the compressional and shear wave velocity respectively, which are obtained from Navier's equation [39]

$$v_{\mathrm{l}} = \sqrt{\left(B + \frac{4}{3}G\right)/\rho}, \qquad v_{\mathrm{s}} = \sqrt{G/\rho}. \tag{13}$$

3. Results

3.1. Ground state properties

The calculated ground state properties, i.e., the equilibrium lattice constant and elastic constants, of fluorite-type oxides CeO_2, ThO_2 and PoO_2 are given in tables 1 and 2. The lattice constants agree well with the experimental values. The deviation is less than 1.5%,

Table 1. Calculated lattice constants expressed in angstroms, bulk moduli in gigapascals and B'_0 for CeO_2, ThO_2 and PoO_2, compared with experiment and other theoretical calculations. The bulk moduli have been calculated both at the experimental and theoretical equilibrium volume ($B_0(V_0^{exp})$) and $B_0(V_0^{th})$, respectively).

Compound	Method	Lattice constant	$B_0(V_0^{th})$	$B_0(V_0^{exp})$	B'_0
CeO_2	LDA	5.33	218	181	4.2
	GGA	5.43	184	195	4.2
	Exp	5.41[a]		220(9)[a], 204[h]	5.4(2)[a]
	Others	5.38[a], 5.39[b], 5.48[c], 5.36[j]	214.7[b], 187.7[c], 176.9[a], 210[j]		4.4[j]
ThO_2	LDA	5.52	225	189	4.4
	GGA	5.61	198	204	4.5
	Exp	5.60[d]		195(2)[d], 198(2)[e], 193[i]	4.4(4)[d]
	Others	5.53[f]	221[f]		
PoO_2	LDA	5.46	188	135	4.3
	GGA	5.56	171	159	3.7
	Exp	5.64[g]			

[a] Reference [40], [b] Reference [2], [c] Reference [13], [d] Reference [25], [e] Reference [24], [f] Reference [41], [g] Reference [42], [h] From elastic constants of reference [26], [i] From elastic constants of reference [27], [j] Reference [28].

Table 2. Calculated elastic constants, shear modulus G, Young's modulus E, all expressed in gigapascals, and Poisson's ratio ν for CeO_2, ThO_2 and PoO_2. For C_{44} the values without oxygen relaxation are quoted in parentheses (see text for discussion). The theoretical lattice constant is used.

Compound	Method	C_{11}	C_{12}	C_{44}	G	E	ν
CeO_2	LDA	399.5	127.5	63.5 (115.1)	92.5	243.1	0.314
	GGA	353.8	99.1	51.0 (96.5)	81.5	213.1	0.307
	Exp[a]	403	105	60	96	249	0.297
	Others[b]	386	124	73			
ThO_2	LDA	405.2	134.4	83.7 (148.9)	104.4	271.1	0.299
	GGA	376.0	109.8	68.1 (109.1)	94.1	243.8	0.295
	Exp[c]	367	106	79	100	256	0.279
PoO_2	LDA	342.0	110.8	55.7 (124.7)	79.7	209.4	0.314
	GGA	318.5	97.0	47.0 (103.8)	72.5	190.5	0.314

[a] Reference [26], [b] Reference [28], [c] Reference [27].

with the GGA values slightly better than the LDA values, which are consistently lower than the experimental lattice constants. The calculated bulk modulus for CeO_2 matches well with the results reported in previous theory works [2, 13]. Despite the fact that the LDA usually overestimates the bulk modulus compared to experiment, here in the case of CeO_2 it is in excellent agreement with the experimental value.

In the case of ThO_2 the long debate which existed for nearly two decades regarding the zero-pressure bulk modulus was recently settled by Staun Olsen *et al* [25], and Iridi *et al* [24], and our GGA value is in excellent agreement with the experimental value. As far as PoO_2 is concerned no experimental value for the bulk modulus is available and the present work is the first theoretical prediction for this quantity, $B = 171$ GPa (GGA), which is slightly smaller than found for CeO_2 and ThO_2.

The bulk modulus scales with the volume, and if we use the Murnaghan equation, the expression for the interdependence between the bulk modulus and the volume becomes

particularly simple [43]:

$$B(V) = B(V_0) \left(\frac{V_0}{V}\right)^{B'},$$ (14)

where B' is the pressure derivative of the bulk modulus. Since the calculated equilibrium volumes are overestimated with GGA and underestimated with LDA, an error, solely depending on the error in the volume, is introduced in the result for the bulk modulus. Therefore, we calculated the bulk modulus also at the experimental volume using the equation above; see the rightmost column in table 1. We find that this diminishes the spread between the LDA and GGA results, as expected. In addition, it also causes LDA to give *smaller* bulk modulus than GGA for the systems studied. In the case of CeO_2, we see that the very good agreement with experiment for the LDA bulk modulus evaluated at the theoretical volume actually is due to the underestimation of the equilibrium volume. For ThO_2, our calculated bulk moduli at the experimental volume converge around the experimental values, with a deviation from the experimental value of about 5%.

The elastic constants of CeO_2, ThO_2 and PoO_2 calculated in the present work are given in table 2 and compared to experimental values (for CeO_2 and ThO_2). One observes that C_{11} and C_{12} agree quite well with the experimental values. In the present calculation, we moreover find that the elastic constants calculated with the GGA are in better agreement with the experimental value than those derived on the basis of LDA. One point of caution is the fact that the calculated values pertain to 0 K temperature, while experiments are performed at room temperature. Finite temperature generally tends to reduce the elastic constants. Consequently, we expect the experimental values at low temperature to be somewhat larger than the values quoted in table 2.

The calculation of C_{44} is particularly delicate. In the fluorite-type structure the anion occupies the tetrahedral position, which when subjected to the monoclinic strain, equation (6), allows for additional relaxation given by an internal parameter, which must be optimized by energy minimization. This leads to a smaller C_{44} compared to the unrelaxed case, and the reduction can be quite substantial [45]. In table 2 we compare the relaxed and unrelaxed values for CeO_2, ThO_2 and PoO_2. Indeed, a large effect is also found in the present cases, with C_{44} reducing approximately by a factor of two compared to the unrelaxed case. Among the actinide dioxides theoretical calculations of elastic constants are available only for UO_2 [44], and this work also found a theoretical C_{44} value more than twice as large as the experimental value, presumably because oxygen relaxation was not included.

Using the calculated elastic constants in table 2, we have derived the average sound velocities and Debye temperatures for CeO_2, ThO_2 and PoO_2; see table 3. The Debye temperature is calculated from the average elastic wave velocity, cf equation (11), the density and the molecular weight of the above compounds are taken from [46, 47]. The calculated values seem to overestimate the experimental Debye temperatures of references [48, 49] by $\sim$30 %; however, when the experimental elastic constants are used in equations (11)–(13), the agreement is considerably better.

3.2. Electronic structure

The electronic structures of CeO_2 and ThO_2 have already been discussed earlier in many other works; see, e.g. [2, 41]. Hence, we concentrate on the compound PoO_2 about which nothing has been reported so far. The band structure of PoO_2 is shown in figures 1 and 2 with and without spin–orbit interaction included, respectively, while figure 3 shows the density of states in the case of spin–orbit interaction being included. PoO_2 is a peculiar oxide, as both Po and O belong
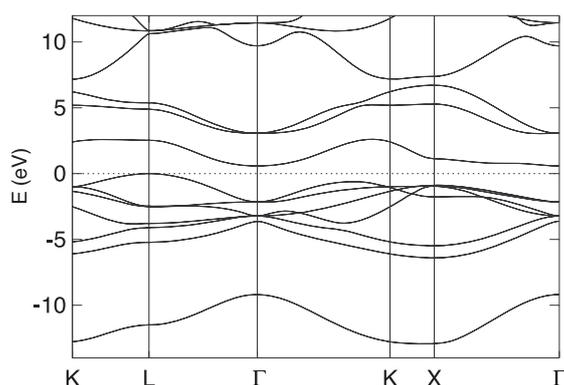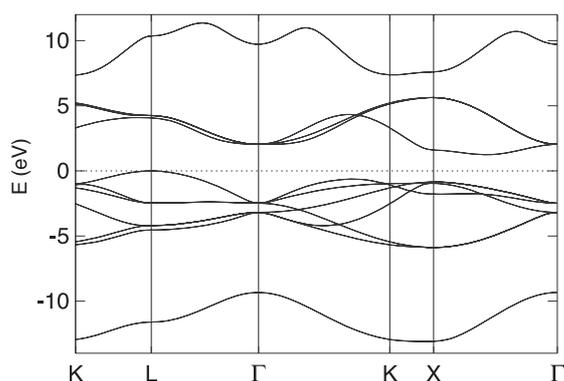
Figure 1. Band structure of PoO$_2$ including spin–orbit interaction. The energy is set to zero at the valence band top.

Table 3. Calculated longitudinal, shear, and average wave velocity (v_l, v_s, and v_m, respectively) in m s^{-1} and the Debye temperature θ_D in kelvins from the average elastic wave velocity for CeO$_2$, ThO$_2$ and PoO$_2$. The theoretical lattice constant is used.

Compound	Method	v_l	v_s	v_m	θ_D
CeO$_2$	LDA	6876	3579	4005	349.8
	GGA	6366	3360	3756	328.1
	Exp				480[a], 355[b]
ThO$_2$	LDA	6035	3232	3610	304.7
	GGA	5695	3069	3426	289.1
	Exp				370[c], 297[d]
PoO$_2$	LDA	5740	2987	3343	280.1
	GGA	5474	2850	3189	267.2

[a] Reference [48], [b] Calculated using equations (11)–(13) with elastic constants from reference [26],
[c] Reference [49], [d] Calculated using equations (11)–(13) with elastic constants from reference [27].

to the sixth group of the periodic table. However, due to the electronegativity of O, Po is rather to be considered a tetravalent cation, which donates its four 6p electrons to the O anions. This is reflected in the band structure in figure 1 and the concordant density of states in figure 3, which together reveal that PoO$_2$ is a semiconductor, with an indirect band gap. The valence band maximum (VBM) occurs at the zone boundary L point, while the conduction band minimum occurs at the zone centre. The Po 6s band appears as a single isolated band about 12 eV below the VBM, while the O 2p valence bands appear in the region from -6 to 0 eV below the VBM. The O 2p bands are separated from the Po 6p bands by a band gap of 0.60 eV. The partial densities of states also included in figure 3 reveal a significant Po admixture into the O 2p bands; hence a considerable degree of covalency is present. In particular, the lowest part of the O 2p valence band has a significant bonding contribution from Po 6p, with the corresponding antibonding component in the Po 6p bands above the VBM, which in fact has close to equal weight on Po and O. The effect of spin–orbit interaction is elucidated by comparison of figures 1 and 2. In essence, only the Po 6p states feel the spin–orbit interaction leading to a downshift of both the lowest valence band and the lowest conduction band. Without spin–orbit interaction the PoO$_2$ gap is 1.56 eV. Spin–orbit interaction increases the width of the valence bands by 0.2 to 6.4 eV. The O 2s states are not shown in figures 1 and 2, but appear at -16 to -19 eV, cf figure 3.

Figure 2. Band structure of PoO_2 without spin–orbit interaction. The energy is set to zero at the valence band top.
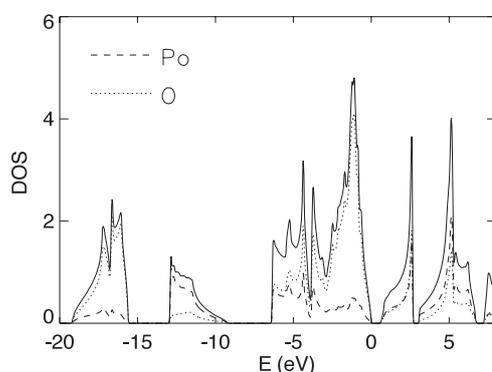
Figure 3. Density of states (DOS) of PoO_2 including spin–orbit interaction. Units are: states per eV and per formula unit. The DOS projected onto the Po site is shown by a dashed line, and the DOS projected onto the O sites with a dotted line. The energy is set to zero at the valence band maximum.

4. Conclusions

In this paper, we have studied the ground state and elastic properties of CeO_2, ThO_2 and PoO_2 using the full-potential linear muffin-tin orbital method within the local density approximation as well as generalized gradient approximation to the exchange correlation potential. For CeO_2 and ThO_2, the calculated ground state properties, such as the lattice constant, bulk modulus, elastic constants, and Debye temperatures, agree well with the experimental values. For PoO_2 the present work is the first quantitative prediction of its elastic properties, which we hope will stimulate experimental investigations. PoO_2 is predicted to be a semiconductor with an indirect band gap.

Acknowledgments

References

[1] Eyring L 1967 Fluorite-related oxide phases of rare earth and actinide elements *Lanthanide/Actinide Chemistry* ed P R Fields and T Moeller (Washington, DC: American Chemical Society)
[2] Skorodumova N V, Ahuja R, Simak S I, Abrikosov I A, Johansson B and Lundqvist B I 2001 *Phys. Rev.* B **64** 115108
[3] Skorodumova N V, Simak S I, Lundqvist B I, Abrikosov I A and Johansson B 2002 *Phys. Rev. Lett.* **89** 166601
[4] Skorodumova N V, Baudin M and Hermansson K 2004 *Phys. Rev.* B **69** 075401
[5] Mamontov E, Egami T, Dmowski W and Kao C C 2001 *J. Phys. Chem. Solids* **62** 819
[6] Wang A Q and Golden T D 2003 *J. Electrochem. Soc.* **150** C616
[7] Inaba H and Tagawa H 1996 *Solid State Ion.* **83** 1
[8] Andersson D A, Simak S I, Skorodumova N V, Abrikosov I A and Johansson B 2006 *Proc. Natl Acad. Sci.* **103** 3518
[9] Linares R C 1967 *J. Phys. Chem. Solids* **28** 1285
[10] Yang Z, Woo T K, Baudin M and Hermansson K 2004 *J. Chem. Phys.* **120** 7741
[11] Gennard S, Corá F and Catlow C R A 1999 *J. Phys. Chem.* B **103** 10158
[12] Koelling D D, Boring A M and Wood J H 1983 *Solid State Commun.* **47** 227
[13] Fabris S, de Gironcoli S, Baroni S, Vicario G and Balducci G 2005 *Phys. Rev.* B **71** 041102(R)
[14] Petit L, Svane A, Szotek Z and Temmerman W M 2005 *Phys. Rev.* B **72** 205118
[15] Hanyu T, Ishii H, Yanagihara M, Kamada T, Miyahara T, Kato H, Naito K, Suzuki S and Ishii T 1985 *Solid State Commun.* **56** 381
[16] Wuilloud E, Delley B, Schneider W-D and Baer Y 1984 *Phys. Rev. Lett.* **53** 202
[17] Karnatak R C, Esteva J-M, Dexpert H, Gasgnier M, Caro P E and Albert L 1987 *Phys. Rev.* B **36** 1745
   Dexpert H, Karnatak R C, Esteva J-M, Connerade J P, Gasgnier M, Caro P E and Albert L 1987 *Phys. Rev.* B **36** 1750
[18] Fujimori A 1983 *Phys. Rev.* B **28** 2281
[19] Hague C F, Mariot J-M, Delaunay R, Gallet J-J, Journel L and Rueff J-P 2004 *J. Electron. Spectrosc. Relat. Phenom.* **136** 179
[20] Liu L-G 1980 *Earth Planet. Sci. Lett.* **49** 166
[21] Duclos S J, Vohra Y K, Ruoff A L, Jayaraman A and Espinosa G P 1988 *Phys. Rev.* B **38** 7755
[22] Kourouklis G A, Jayaraman A and Espinosa G P 1988 *Phys. Rev.* B **37** 4250
[23] Jayaraman A, Kourouklis G A and Vanultert L G 1988 *Pramana J. Phys.* **30** 225
[24] Iridi M, Le Bihan T, Heathman S and Rebizant J 2004 *Phys. Rev.* B **70** 014113
[25] Olsen J S, Gerward L, Kanchana V and Vaitheeswaran G 2004 *J. Alloys Compounds* **381** 37
[26] Nakajima A, Yoshihara A and Ishigma M 1994 *Phys. Rev.* B **50** 13297
[27] Macedo P M, Capps W and Watchman J B 1964 *J. Am. Ceram. Soc.* **47** 651
[28] Gürel T and Eryiġit R 2006 *Phys. Rev.* B **74** 014302
[29] Savrasov S Y 1996 *Phys. Rev.* B **54** 16470
[30] Vosko S H, Wilk L and Nusair M 1980 *Can. J. Phys.* **58** 1200
[31] Perdew J P, Burke K and Ernzerhof M 1996 *Phys. Rev. Lett.* **77** 3865
[32] Birch F J 1938 *J. Appl. Phys.* **9** 279
[33] Nordström L, Wills J M, Andersson P H, Söderlind P and Eriksson O 2000 *Phys. Rev.* B **63** 035103
   Delin A and Klüner T 2002 *Phys. Rev.* B **66** 035117
[34] Wallace D C 1972 *Thermodynamics of Crystals* (New York: Wiley)
[35] Dacorogna M, Ashkenazi J and Peter M 1982 *Phys. Rev.* B **26** 1527
[36] Christensen N E 1984 *Solid State Commun.* **49** 701
[37] Liu A Y and Singh D J 1993 *Phys. Rev.* B **47** 8515
[38] Anderson O L 1996 *J. Phys. Chem. Solids* **24** 909
[39] Schreiber E, Anderson O L and Soga N 1973 *Elastic Constants and their Measurements* (New York: McGraw-Hill)
[40] Gerward L, Staun Olsen J, Petit L, Vaitheeswaran G, Kanchana V and Svane A 2005 *J. Alloys Compounds* **400** 56–61
[41] Li S, Ahuja R and Johansson B 2002 *High Pressure Res.* **22** 471
[42] Villars P and Calvert L D 1991 *Pearson's Handbook of Crystallographic Data for Intermetallic Phases* 2nd edn (Metals Park, OH: ASM International)
[43] Delin A, Fast L, Johansson B, Eriksson O and Wills J M 1998 *Phys. Rev.* B **58** 4345
[44] Dudarev S L, Botton G A, Savrasov S Y, Szotek Z, Temmerman W M and Sutton A P 1998 *Phys. Status Solidi* a **166** 429

[45] Mérawa M, Llunell M, Orlando R, Gelize-Duvignau M and Dovesi R 2003 *Chem. Phys. Lett.* **368** 7
[46] Weast R C (ed) 1981 *CRC Handbook of Chemistry and Physics* 62nd edn (Boca Raton, FL: CRC press)
[47] Lide D R (ed) 1998 *CRC Handbook of Chemistry and Physics* 79th edn (Boca Raton, FL: CRC press)
[48] Hisashige T, Yamamura Y and Tsuji T 2006 *J. Alloys Compounds* **408–412** 1153
[49] White G K and Sheard F W 1974 *J. Low Temp. Phys.* **14** 445